JOURNAL OF NATURAL PRODUCTS

pubs.acs.org/jnp

Article

Ravidomycin Analogs from *Streptomyces* sp. Exhibit Altered Antimicrobial and Cytotoxic Selectivity

Kyoung Jin Park,* Sarah Maier, Chengqian Zhang, Shelley A. H. Dixon, Douglas B. Rusch, Monica T. Pupo, Steven P. Angus, and Joseph P. Gerdt*

Cite This: *J. Nat. Prod.* 2023, 86, 1968−1979

Read Online

ACCESS | Metrics & More | Article Recommendations | Supporting Information

ABSTRACT: Six new ravidomycin analogs (**1**−**4**, **6**, and **7**) were isolated from *Streptomyces* sp. Am59 using UV- and LCMS-guided separation based on Global Natural Products Social (GNPS) molecular networking analysis. Furthermore, we isolated fucomycin V (**9**), which possesses the same chromophore as ravidomycin but features a D-fucopyranose instead of D-ravidosamine. This is the first report of **9** as a natural product. Four new analogs (**10**−**13**) of **9** were also isolated. The structures were elucidated by combined spectroscopic and computational methods. We also found an inconsistency with the published $[\alpha]_D^{25}$ of deacetylravidomycin, which is reported to have a (−) sign. Instead, we observed a (+) specific rotation for the reported absolute configuration of deacetylravidomycin (containing D-ravidosamine). We confirmed the positive sign by reisolating deacetylravidomycin from *S. ravidus* and by deacetylating ravidomycin. Finally, antibacterial, antifungal, and cytotoxicity activities were determined for the compounds. Compared to deacetylravidomycin, the compounds **4**−**6**, **9**, **11**, and **12** exhibited greater antibacterial selectivity.

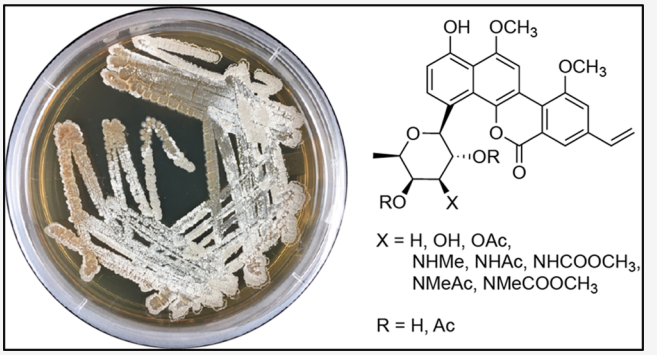

The ravidomycin/gilvocarcin/chrysomycin group of angucyclines is produced via type II polyketide synthases (PKS) and exhibits potent antitumor and antibiotic activity.[1] Their activity is uniquely promoted by UV and visible light, owing to the ability of their conserved benzo[*d*]naphtho[1,2-*b*]pyran-6-one moiety to covalently modify thymine residues in DNA via a photoactivated [2 + 2] cycloaddition.[2,3] Numerous analogs have been discovered[4−9] and synthesized[10] with different sugars or variations of the aglycone. The identity of the sugar moiety strongly contributes to their activity.[11,12] The vinyl group of the aglycone is also important for toxicity.[12−14]

Ravidomycin, which contains the amino sugar ravidosamine, was first reported for its strong antibiotic effects from *Streptomyces ravidus* in 1980,[15] but its chemical structure was established in 1981.[16] Subsequently, a few new congeners have been isolated,[5,6,17] and total syntheses of ravidomycin and deacetylravidomycin M have been reported.[18,19] Although there have been no comprehensive direct structure−activity relationship (SAR) experiments of ravidomycin analogs, ravidomycin and deacetylravidomycin have shown potent antitumor and antibiotic activity.[17,20,21]

Molecular networking analysis[22] revealed that new analogs of ravidomycin were produced by a bacterial strain (*Streptomyces* sp. Am59), which was isolated from a fungus in Brazil. From this strain, six new ravidomycin-type analogs (**1**−**4**, **6**, and **7**), six known ravidomycin-type analogs (**5**, **8**, and **14**−**17**), fucomycin V (**9**), and four new fucomycin analogs (**10**−**13**) were characterized, and their antibacterial, antifungal, and cytotoxic activities were determined. We also believe that we identified an error in the published specific rotation of deacetylravidomycin, which is reported to have a (−) sign.[6] We instead found the specific rotation of this compound to have a (+) sign, which we confirmed by reisolating deacetylravidomycin from the original producer, *S. ravidus*, and by chemically deacetylating pure ravidomycin. Here, the isolation, structural elucidation, and biological activities of these ravidomycin analogs are described.

RESULTS AND DISCUSSION

Molecular Networking and UV−vis Spectroscopy Reveal Previously Unreported Analogs of Ravidomycin.

Streptomyces sp. AM59 was isolated from a fungus in Brazil and cultured in three different liquid media. The combined chemical extracts from the supernatants were examined by LC-MS/MS and subjected to molecular networking using the Global Natural Products Social (GNPS) platform.[22] A six-

Received: May 4, 2023
Published: August 2, 2023

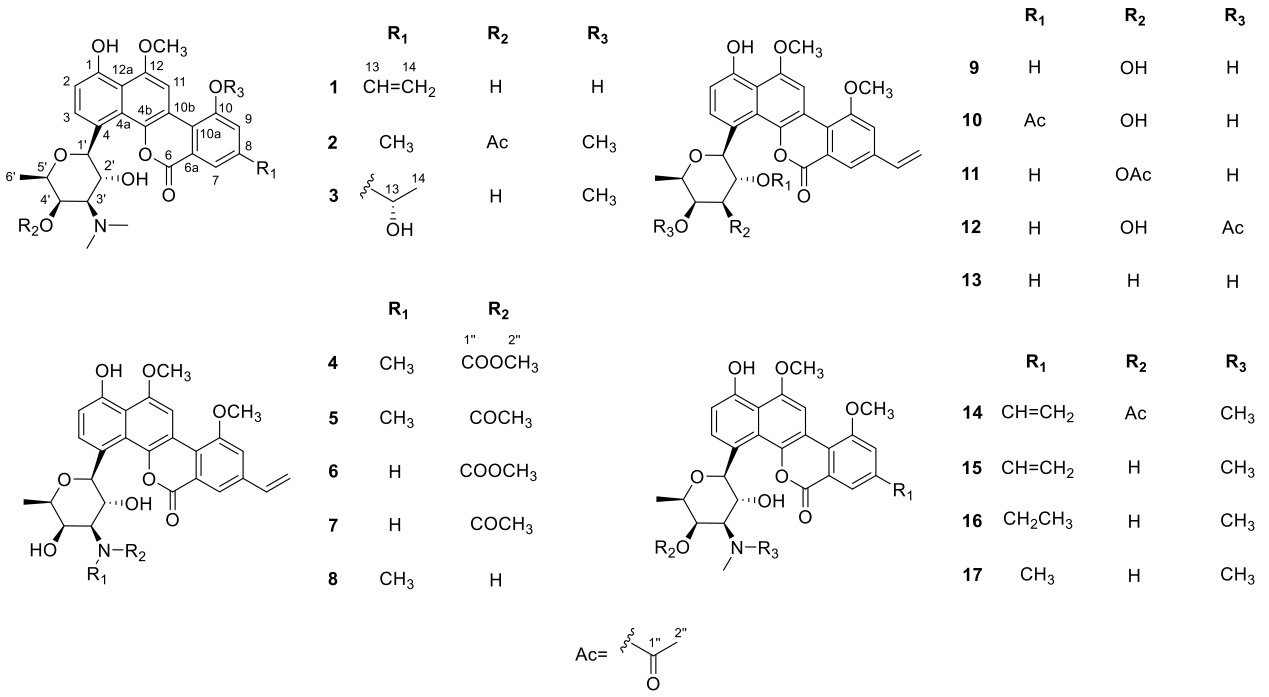

member cluster contained a precursor ion of 564.2227 *m/z*, which matched the $[M + H]^+$ ion for ravidomycin[16] present in the NPAtlas database (Figure 1A).[23] The UV−vis absorbance

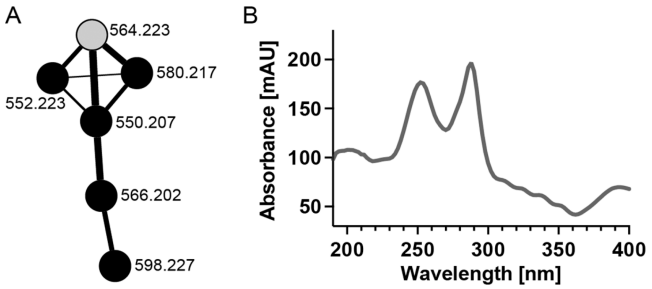

Figure 1. Ravidomycin analogs observed. (A) Molecular networking in GNPS revealed a cluster containing ravidomycin (gray node, 564.223 *m/z*) and five analogs. Nodes are labeled with the *m/z* of the precursor ion. (B) UV−vis absorbance spectrum for ravidomycin.

spectrum for this molecule matched that of ravidomycin (Figure 1B).[17,20] Therefore, this cluster likely comprised ravidomycin and multiple ravidomycin analogs. The chemical extract of this bacterial supernatant revealed several more peaks with UV−vis absorbance spectra similar to that of ravidomycin, some of which had monoisotopic masses that did not match known ravidomycin analogs. These analogs were targeted for isolation and identification by NMR.

Structure Elucidation of 17 Metabolites Including Six New Ravidomycin and Four New Fucomycin Analogs. 10-*O*-Demethyl-deacetylravidomycin (**1**) was obtained as a yellow amorphous solid. Its molecular formula was established as $C_{28}H_{29}NO_8$ based on HR-ESI-MS. The UV spectrum of **1** matched the angucyclinone-derived tetracyclic aromatic system of ravidomycin,[17] gilvocarcin V,[4] and chrysomycin A.[24] The analysis of ^{1}H NMR data (Table 1) revealed characteristic signals for three aromatic rings including two 1,2,3,4-tetrasubstituted aromatic protons [δ_H 7.96 (H-3) and 7.06 (H-2)], a 1,2,3,4,5-pentasubstituted aromatic proton [δ_H 8.90 (H-11)], and two 1,2,3,5-tetrasubstituted aromatic protons [δ_H 8.01 (H-7) and 7.51 (H-9)]. Additionally, there were three vinyl group protons [δ_H 6.86 (H-13), 5.99 (H-14b), and 5.47 (H-14a)], a dimethyl aminosugar moiety [δ_H 6.17 (H-1′), 4.42 (H-2′), 4.32 (H-5′), 4.29 (H-4′), 3.71 (H-3′), 3.12 (3′-NCH_3 × 2), and 1.32 (H-6′)], and a methoxy group [δ_H 4.21 (12-OCH_3)]. The ^{13}C NMR spectrum (Table 2) displayed 27 of the 28 carbons, including a carbonyl carbon [δ_C 161.0 (C-6)], 15 aromatic carbons [δ_C 154.5 (C-1), 152.4 (C-12), 142.1 (C-4b), 139.3 (C-8), 129.3 (C-3), 125.3 (C-4a), 124.4 (C-4), 122.6 (C-6a), 121.9 (C-10a), 118.4 (C-9), 118.3 (C-7), 115.9 (C-12a), 115.4 (C-10b), 111.9 (C-2), and 102.5 (C-11)], two olefinic methine carbons [δ_C 135.1 (C-13) and 115.4 (C-14)], four oxygenated methine carbons [δ_C 79.3 (C-1′), 75.6 (C-5′), 68.5 (C-4′), and 66.4 (C-2′)], a nitrogenated methine carbon [δ_C 70.1 (C-3′)], a methoxy carbon [δ_C 55.6 (12-OCH_3)], two nitrogenated methyl carbons [δ_C 40.5 (3′-NCH_3 × 2)], and a methyl carbon [δ_C 15.3 (C-6′)]. No HMBC correlations reliably revealed C-10 in this congener. The NMR spectroscopic data indicated that this compound was ravidomycin-like with an aminosugar as a *C*-glycoside.[5,6,17] These data were close to those of deacetylravidomycin (**15**),[6] except for the presence of a hydroxy group instead of a methoxy group (δ_C 56.0) at C-10. The remaining methoxy group is bound to C-12, as evidenced by the HMBC correlation (Figure 2) between the methoxy protons (δ_H 4.21) and C-12 (δ_C 152.4) and the NOESY correlation (Figure 3A) between the methoxy protons (δ_H 4.21) and H-11 (δ_H 8.90). The planar structure of **1** was fully determined from 2D NMR spectroscopic data including COSY, HSQC, and HMBC (Figure 2).

Ravidomycin M (**2**) was obtained as a yellow amorphous solid with molecular formula $C_{30}H_{33}NO_9$ based on HR-ESI-MS. The NMR data of **2** showed a methyl group (δ_C 20.1; δ_H 2.52) instead of a vinyl group (δ_C 135.2; δ_H 6.76 and δ_C 116.2; δ_H 5.91 and 5.44) at C-8 in ravidomycin (**14**).[17] The spectra also resembled those of deacetylravidomycin M (**17**),[6] except with acetylation of C-4′, which is evident from an HMBC correlation (Figure 2) from H-4′ to C-1″.

https://doi.org/10.1021/acs.jnatprod.3c00381
J. Nat. Prod. 2023, 86, 1968−1979

Table 1. ^{1}H NMR (500 MHz) [ppm, mult., (J in Hz)] Spectroscopic Data of Compounds 1−7 in Methanol-d_4

pos.	1	2	3	4a	4b	5a	5b	6	7
2	7.06 (1H, d, 8.4)	7.03 (1H, d, 8.4)	7.06 (1H, d, 8.4)	7.00 (1H, d, 8.4)	7.00 (1H, d, 8.4)	7.01 (1H, d, 8.4)	7.01 (1H, d, 8.4)	7.00 (1H, d, 8.3)	7.01 (1H, d, 8.3)
3	7.96 (1H, d, 8.4)	7.91 (1H, d, 8.4)	7.96 (1H, d, 8.4)	7.95 (1H, d, 8.4)	7.95 (1H, d, 8.4)	7.96 (1H, overlapped)	7.96 (1H, overlapped)	7.87 (1H, d, 8.3)	7.89 (1H, d, 8.3)
7	8.01 (1H, brs)	7.83 (1H, brs)	8.10 (1H, d, 1.7)	7.97 (1H, brs)	7.96 (1H, brs)	7.95 (1H, overalpped)	7.95 (1H, overalpped)	8.10 (1H, s)	8.14 (1H, s)
9	7.51 (1H, brs)	7.38 (1H, brs)	7.68 (1H, d, 1.7)	7.48 (1H, brs)	7.46 (1H, brs)	7.46 (1H, brs)	7.47 (1H, brs)	7.65 (1H, s)	7.70 (1H, s)
11	8.90 (1H, s)	8.55 (1H, s)	8.72 (1H, s)	8.38 (1H, s)	8.37 (1H, s)	8.37 (1H, s)	8.39 (1H, s)	8.61 (1H s)	8.68 (1H s)
13	6.86 (1H, dd, 17.5, 10.9)	2.52 (3H, s)	5.05 (1H, q, 6.6)	6.83 (1H, overlapped)	6.83 (1H, overlapped)	6.80 (1H, overlapped)	6.80 (1H, overlapped)	6.93 (1H, dd, 17.6, 10.9)	6.95 (1H, dd, 17.6, 11.0)
14a	5.47 (1H, d, 10.9)		1.57 (3H, d, 6.6)	5.46 (1H, d, 10.9)	5.45 (1H, d, 10.9)	5.45 (1H, d, 10.8)	5.45 (1H, d, 10.8)	5.50 (1H, d, 10.9)	5.51 (1H, d, 11.0)
14b	5.99 (1H, d, 17.5)			6.01 (1H, d, 17.6)	6.00 (1H, d, 17.6)	6.00 (1H, d, 17.6)	6.00 (1H, d, 17.6)	6.08 (1H, d, 17.6)	6.10 (1H, d, 17.6)
1′	6.17 (1H, d, 9.1)	6.10 (1H, d, 9.0)	6.15 (1H, d, 9.1)	6.02 (1H, d, 9.4)	6.05 (1H, d, 9.4)	6.07 (1H, d, 9.0)	6.11 (1H, d, 9.0)	5.97 (1H, d, 9.6)	5.99 (1H, d, 9.1)
2′	4.42 (1H, t, 9.7)	4.41 (1H, overlapped)	4.40 (1H, t, 9.7)	4.41 (1H, overlapped)	4.47 (1H, t, 9.7)	4.50 (1H, t, 9.7)	4.38 (1H, t, 9.7)	4.13 (1H, t, 9.6)	4.19 (1H, overlapped)
3′	3.71 (1H, brd, 10.8)	3.64 (1H, brd, 10.8)	3.67 (1H, dd, 10.5, 2.9)	4.30 (1H, brd, 10.7)	4.38 (1H, brd, 10.7)	4.76 (1H, brd, 10.7)	4.17 (1H, brd, 10.7)	3.97 (1H, brd, 9.6)	4.24 (1H, overlapped)
4′	4.29 (1H, overlapped)	5.67 (1H, brs)	4.27 (1H, overlapped)	3.93 (1H, brs)	3.96 (1H, brs)	3.95 (1H, brs)	3.99 (1H, brs)	3.84 (1H, brs)	3.84 (1H, brs)
5′	4.32 (1H, overlapped)	4.45 (1H, overlapped)	4.29 (1H, overlapped)	4.36 (1H, overlapped)	4.42 (1H, overlapped)	4.43 (1H, q, 6.5)	4.35 (1H, q, 6.5)	4.45 (1H, q, 6.5)	4.45 (1H, q, 6.5)
6′	1.32 (3H, overlapped)	1.13 (3H, d, 6.4)	1.30 (3H, d, 6.4)	1.24 (3H, d, 6.5)	1.24 (3H, d, 6.5)	1.23 (3H, d, 6.5)	1.28 (3H, d, 6.5)	1.23 (3H, d, 6.5)	1.23 (3H, d, 6.5)
2″		2.24 (3H, s)		3.79 (3H, s)	3.75 (3H, s)	2.20 (3H, s)	2.31 (3H, s)	3.70 (3H, s)	2.07 (3H, s)
10-OCH_3		4.12 (3H, s)	4.22 (3H, s)	4.09 (3H, s)	4.08 (3H, s)	4.09 (3H, s)	4.10 (3H, s)	4.20 (3H, s)	4.22 (3H, s)
12-OCH_3	4.21 (3H, s)	4.16 (3H, s)	4.23 (3H, s)	4.06 (3H, s)	4.05 (3H, s)	4.06 (3H, s)	4.07 (3H, s)	4.17 (3H, s)	4.21 (3H, s)
3′-NCH_3	3.12 (3H, s) × 2	2.80 (3H, s) × 2	3.09 (3H, s) × 2	3.19 (3H, s)	3.18 (3H, s)	3.29 (3H, s)	3.17 (3H, s)		

Deacetylravidomycin HE (**3**) was obtained as a yellow amorphous solid with molecular formula $C_{29}H_{33}NO_9$ based on its HR-ESI-MS spectrum. The ^{1}H and ^{13}C NMR spectra (Tables 1 and 2) of **3** revealed that the signals of an oxygenated methine [δ_C 68.7 (C-13); δ_H 5.05 (H-13)] and a methyl group [δ_C 24.2 (C-14); δ_H 1.57 (H-14)] replaced the signals of a vinyl group [δ_C 135.2 (C-13); δ_H 6.92 (H-13) and δ_C 117.4 (C-14); δ_H 6.13 (H-14b) and 5.48 (H-14a)] at C-8 in **15**.[6] HMBC correlations of H-14 to C-8 and H-9 to C-13 (Figure 2) confirmed the placement of this alcohol side chain at C-8. Therefore, **3** is similar to gilvocarcin HE[7] but with a ravidosamine replacing the fucofuranose.

N-Demethyl-*N*-methoxycarbonyl-deacetylravidomycin (**4**) was isolated as a yellow amorphous solid with molecular formula $C_{30}H_{31}NO_{10}$ based on its HR-ESI-MS spectrum. The ^{1}H NMR spectrum (Table 1) of **4** displayed a 0.9:1 mixture of two methyl carbamate isomers (**4a** and **4b**) that were analogs of **15**. The analysis of 2D NMR spectra (Figure 2) verified that the two isomers had the same planar structure containing a methyl carbamate moiety bound to the nitrogen atom, as evidenced by the HMBC correlations of H-3′ to C-1″ and 3′-NCH_3 to C-3′ and C-1″. Because the largest difference in chemical shift between the isomer signals was observed around C-3′, we believe that these peaks are due to *cis* and *trans* isomers of the carbamate. Generally, asymmetric *N*,*N*-disubstituted amides can exhibit stable *cis* and *trans* isomers in solution—the ratio of which depends on the substituents on the nitrogen and carbonyl groups.[25,26] The NOESY spectrum (Figure 3B) showed a correlation of 3′-NCH_3 (δ_H 3.19) to H-2″ (δ_H 3.79) in **4a** and no correlation between 3′-NCH_3 (δ_H 3.18) and H-2″ (δ_H 3.75) in **4b**, indicating a 4-*Z* (**4a**) to 4-*E* (**4b**) ratio of 0.9:1.

Compound **5** was isolated as a yellow amorphous solid with molecular formula $C_{30}H_{31}NO_9$, as determined by HR-ESI-MS. The comparison of MS spectra and NMR data (Table 1 and Figure 2) to those of **4** showed the loss of an oxygen atom and the presence of a methyl group instead of a methoxy group at C-1″. This compound has been reported as FE35A[5] without any mention of the splitting of the NMR signals due to *cis*/*trans* isomerization of the *N*,*N*-disubstituted amide. We observed peaks with a 2:1 ratio, which is a larger difference than exhibited by **4**. The NOE cross-peaks (Figure 3B) of **5** showed correlations between H-2″ (δ_H 2.20) and 3′-NCH_3 (δ_H 3.29) in **5a** and between H-2″ (δ_H 2.31) and both H-3′ (δ_H 4.17) and H-4′ (δ_H 3.99) in **5b**. Thus, the 5-*Z* (**5a**) to 5-*E* (**5b**) ratio of **5** was 2:1.

N,*N*-Didemethyl-*N*-methoxycarbonyl-deacetylravidomycin (**6**) and *N*,*N*-didemethyl-*N*-acetyl-deacetylravidomycin (**7**) were obtained as yellow amorphous solids. The HR-ESI-MS spectra of **6** and **7** revealed that they have molecular formulas of $C_{29}H_{29}NO_{10}$ and $C_{29}H_{29}NO_9$, respectively, based on HR-ESI-MS. The 1D NMR spectra of **6** and **7** (Tables 1 and 2) displayed similar peak patterns to those of **4** and **5** except for the absence of a methyl group signal (δ_C 30.4 × 2; δ_H 3.19 and 3.18 in **4** and δ_C 29.4 and 32.7; δ_H 3.29 and 3.17 in **5**). The planar structures of **6** and **7** were determined by 2D NMR analysis (Figure 2) to be *N*-monosubstituted analogs of **4** and **5**, respectively. These nonmethylated analogs did not exhibit separate peaks for *cis*/*trans* isomers.

Fucomycin V (**9**) was isolated as a yellow amorphous solid with a molecular formula of $C_{27}H_{26}O_9$ based on HR-ESI-MS.

https://doi.org/10.1021/acs.jnatprod.3c00381
J. Nat. Prod. 2023, 86, 1968−1979

Table 2. ^{13}C NMR (125 Hz) Spectroscopic Data of Compounds 1−7 in Methanol-d_4

pos.	1	2	3	4a	4b	5a	5b	6	7
1	154.5	154.7	154.7	154.5	154.5	154.4	154.5	154.5	154.5
2	111.9	111.6	112.0	111.9	111.9	112.0	111.9	111.9	112.0
3	129.3	129.1	129.4	129.5	129.5	129.2	129.5	129.6	129.6
4	124.4	124.5	124.4	125.4	125.4	125.4	125.4	125.1	125.3
4a	125.3	125.1	125.3	125.5	125.5	125.8	125.4	125.5	126.0
4b	142.1	140.7	142.5	142.6	142.6	142.5	142.6	142.7	142.7
6	161.0	160.9	161.0	160.6	160.6	160.8	160.6	160.5	160.8
6a	122.6	121.7	122.6	123.2	123.2	122.2	122.2	122.4	122.6
7	118.3	121.3	118.0	119.0	119.0	119.01	118.99	119.1	119.3
8	139.3	140.7	149.4	139.2	139.2	139.2	139.2	139.3	139.7
9	118.4	118.4	114.9	114.1	114.1	114.2	114.1	114.4	114.4
10	ND[a]	157.4	157.8	157.60	157.57	157.6	157.6	157.8	158.0
10a	121.9	121.3	122.7	123.1	123.1	123.2	123.1	123.4	123.6
10b	115.4	115.3	114.8	114.2	114.2	113.88	113.91	114.4	114.6
11	102.5	102.1	102.3	101.8	101.8	101.7	101.8	102.0	102.2
12	152.4	152.2	152.4	152.11	152.06	152.1	152.1	152.4	152.4
12a	115.9	115.5	115.6	115.6	115.6	115.61	115.64	115.9	115.9
13	135.1	20.1	68.7	135.2	135.2	135.13	135.15	135.4	135.2
14	115.4		24.2	115.7	115.7	115.61	115.64	115.9	115.7
1′	79.3	79.7	79.3	80.0	80.0	80.1	80.0	79.5	79.5
2′	66.4	66.6	66.6	66.4	65.9	67.2	66.1	68.5	68.5
3′	70.1	68.3	70.1	62.9	63.3	65.2	61.5	59.5	58.0
4′	68.5	70.0	68.3	73.7	73.2	74.0	72.8	71.4	71.1
5′	75.6	74.7	75.8	75.7	75.7	76.1	75.7	75.3	75.3
6′	15.3	15.6	15.3	15.7	15.7	15.6	15.6	15.6	15.6
1″		170.7		158.4	158.4	173.17	173.24	158.2	172.4
2″		19.8		52.0	51.9	20.7	21.1	51.1	21.3
10-OCH_3		55.5	55.6	55.6	55.6	55.6	55.6	55.6	55.6
12-OCH_3	55.6	55.5	55.6	55.4	55.4	55.4	55.4	55.5	55.5
3′-NCH_3	40.5 × 2	40.1 × 2	40.3 × 2	30.4	30.4	29.4	32.7		

[a]Not detected.

The spectroscopic data analysis identified that **9** is a ravidomycin-type structure with a D-fucopyranoside instead of a D-ravidosamine. This structure has been previously reported as a synthetic product with significant antituberculosis activity but without detailed structural assignment.[10] Here, we report the first natural isolation of **9** and its full NMR assignment (Table 3 and Figure 2). The 1D and 2D NMR data of **9** showed similar signals to those of **15**[6] with differences in the sugar moiety: five oxygenated methines [δ_C 78.3 (C-1′); δ_H 5.89 (H-1′), δ_C 70.6 (C-2′); δ_H 4.15 (H-2′), δ_C 76.2 (C-3′); δ_H 3.82 (H-3′), δ_C 72.7 (C-4′); δ_H 3.85 (H-4′), and δ_C 74.8 (C-5′); δ_H 4.38 (H-5′)] and one methyl group [δ_C 15.8 (C-6′); δ_H 1.26 (H-6′)].

2′-Acetyl-fucomycin V (**10**), 3′-acetyl-fucomycin V (**11**), and 4′-acetyl-fucomycin V (**12**) were isolated as yellow amorphous solids with the molecular formula $C_{29}H_{28}O_{10}$ based on HR-ESI-MS. Because these compounds had the same monoisotopic mass but different retention times (**10**, 24.8 min; **11**, 23.3 min; **12**, 23.5 min), we expected them to be isomers. The molecular formula of these isomers matches an acetylated version of compound **9**. Indeed, the 1D NMR spectra (Table 3) revealed that each compound had an additional acetyl group compared to **9** {[**10**, δ_C 170.4 (C-1″) and 19.0 (C-2″); δ_H 1.46 (H-2″)], [**11**, δ_C 171.4 (C-1″) and 19.7 (C-2″); δ_H 2.19 (H-2″)], and [**12**, δ_C 171.5 (C-1″) and 19.5 (C-2″); δ_H 2.08 (H-2″)]}. Furthermore, the spectra exhibited downfield-shifted ^{1}H and ^{13}C NMR resonances at different positions of the fucopyranose {[**10**, δ_C 74.1 (C-2′); δ_H 5.35 (H-2′) compared to **9**, δ_C 70.6 (C-2′); δ_H 4.15 (H-2′)], [**11**, δ_C 79.0 (C-3′); δ_H 5.09 (H-3′) compared to **9**, δ_C 76.2 (C-3′); δ_H 3.82 (H-3′)], and [**12**, δ_C 74.6 (C-4′); δ_H 5.23 (H-4′) compared to **9**, δ_C 72.7 (C-4′); δ_H 3.85 (H-4′)]}. These results suggest that the isomers are acetylated at the three different hydroxy groups of the sugar moiety in **9**. The locations of the acetyl groups of **10**−**12** were further established via analysis of the HSQC and HMBC spectra (Figure 2). The HMBC correlations of H-2′ to C-1″ in **10**, H-3′ to C-1″ in **11**, and H-4′ to C-1″ in **12** indicated that the acetyl moiety is connected at C-2′, C-3′, and C-4′ of **10**−**12**, respectively.

3′-Deoxy-fucomycin V (**13**) was purified as a yellow amorphous solid with the molecular formula $C_{27}H_{26}O_8$ based on HR-ESI-MS. This formula has lost one oxygen atom relative to compound **9**. The 1D NMR spectra (Table 3) were similar to compound **9** except for the presence of a methylene [δ_C 42.4 (C-3′); δ_H 2.42 (H-3′b) and 1.71 (H-3′a)] in **13** instead of an oxygenated methine [δ_C 76.2 (C-3′); δ_H 3.82 (H-3′)] in **9**. Analysis of the 2D NMR further confirmed that the structure of **13** contains a fucopyranoside that is deoxygenated at C-3′.

Known congeners were identified as SS50905B (**8**),[27] ravidomycin (**14**),[28] deacetylravidomycin (**15**),[6] dihydrodeacetylravidomycin (**16**),[21] and deacetylravidomycin M (**17**)[6] by comparison of spectroscopic data with previous reports.

Sugar Relative Configuration Is the Same in Each Analog. The relative configurations of the sugar moieties in

https://doi.org/10.1021/acs.jnatprod.3c00381
J. Nat. Prod. 2023, 86, 1968−1979

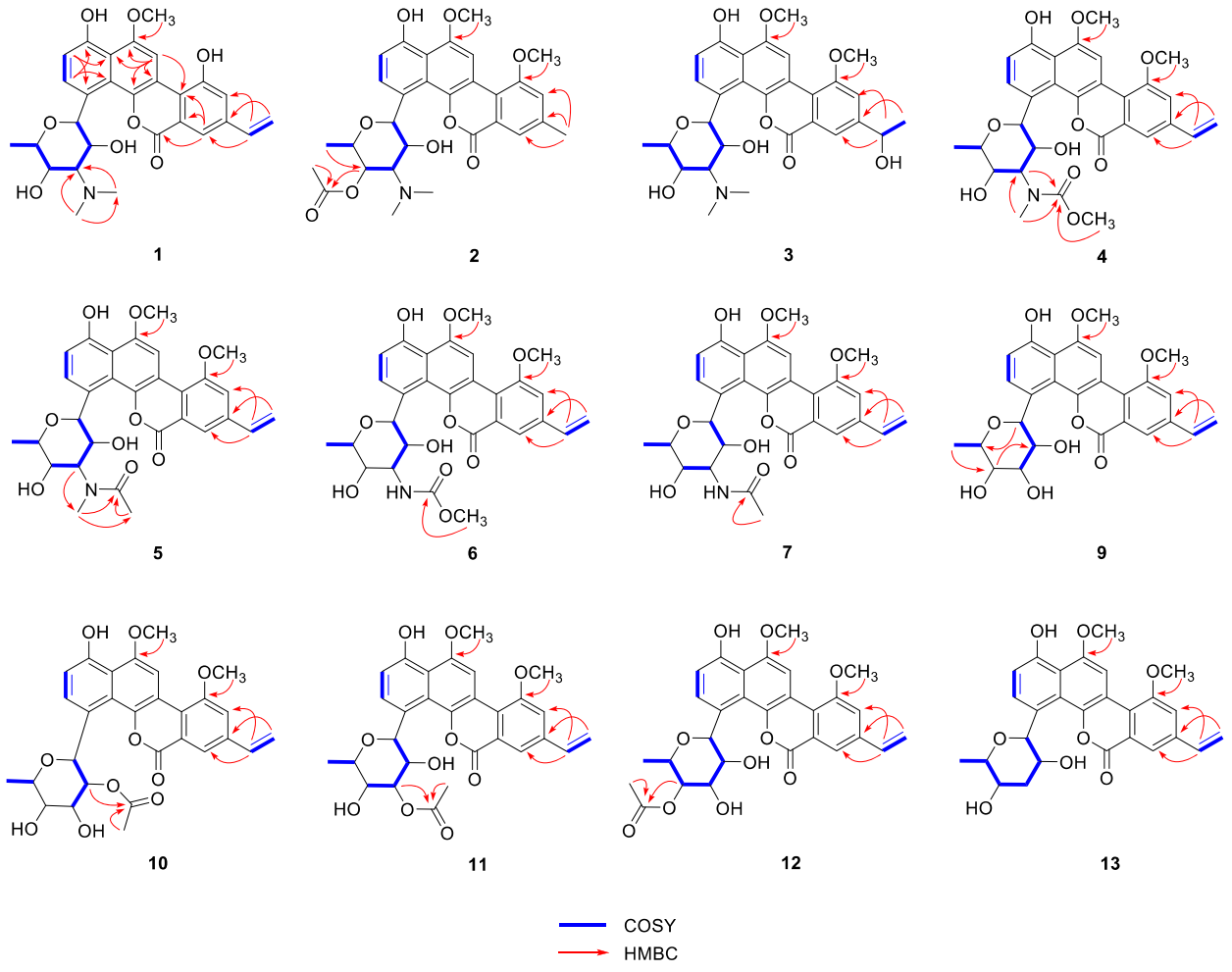

Figure 2. Key COSY and HMBC correlations of **1**−**7** and **9**−**13**.

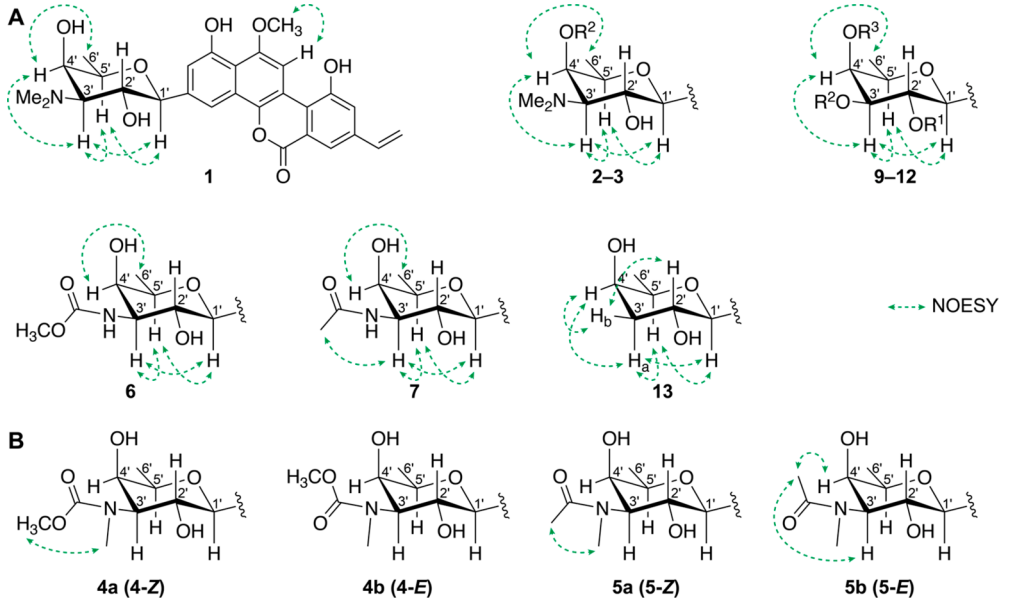

Figure 3. Key NOESY correlations of **1**−**7** and **9**−**13**. (A) NOE correlations of **1**−**3**, **6**, **7**, and **9**−**13**. (B) NOE correlations of **4a**, **4b**, **5a**, and **5b**.

compounds **1**−**7** and **9**−**13** were assigned from NOESY spectroscopic data (Figure 3A). The NOE correlations of H-1′ to both H-3′ and H-5′, as well as the NOE correlations of H-5′ to both H-3′ and H-4′ suggested that H-1′,3′,5′ and H-4′ were cofacial. Furthermore, the NOE correlation of H-4′ to H-6′ suggested that H-4′ and CH_3-6′ were equatorial. **13** also had

https://doi.org/10.1021/acs.jnatprod.3c00381
J. Nat. Prod. 2023, 86, 1968−1979

Table 3. ^{13}C (125 MHz) and ^{1}H (500 MHz) [ppm, mult., (J in Hz)] NMR Spectroscopic Data of Compounds 9−13 in Methanol-d_4

	9		10		11		12		13	
pos.	δ_C	δ_H	δ_C	δ_H	δ_C	δ_H	δ_C	δ_H	δ_C	δ_H
1	154.5		154.3		154.5		154.5		154.5	
2	111.9	7.01 (1H, d, 8.4)	112.3	6.97 (1H, d, 8.4)	111.8	6.99 (1H, d, 8.4)	111.7	6.85 (1H, d, 8.4)	111.9	6.88 (1H, d, 8.4)
3	129.7	7.91 (1H, d, 8.4)	129.3	7.93 (1H, d, 8.4)	129.5	7.89 (1H, d, 8.4)	129.3	7.72 (1H, d, 8.4)	129.3	7.71 (1H, d, 8.4)
4	125.1		124.7		124.6		124.5		125.5	
4a	125.5		124.4		125.4		125.3		125.7	
4b	142.7		142.3		142.5		142.3		142.7	
6	160.8		160.5		160.7		160.6		160.5	
6a	122.4		122.4		122.1		121.9		122.4	
7	119.1	8.08 (1H, brs)	119.1	8.10 (1H, brs)	118.9	7.98 (1H, brs)	118.9	7.77 (1H, d, 1.6)	119.1	7.99 (1H, brs)
8	139.1		139.7		139.2		139.1		139.3	
9	114.4	7.63 (1H, brs)	114.4	7.66 (1H, brs)	114.2	7.51 (1H, brs)	114.0	7.27 (1H, d, 1.6)	114.4	7.55 (1H, brs)
10	157.8		158.0		157.6		157.4		157.8	
10a	123.4		123.4		123.1		122.9		123.4	
10b	114.2		114.2		114.0		113.9		114.2	
11	102.0	8.59 (1H, s)	101.8	8.60 (1H, s)	101.8	8.43 (1H, s)	101.7	8.14 (1H, s)	102.2	8.53 (1H, s)
12	152.4		152.4		152.1		151.9		152.4	
12a	115.9		115.4		115.7		115.6		115.9	
13	135.2	6.91 (1H, dd, 17.5, 10.9)	135.1	6.93 (1H, dd, 17.5, 10.9)	135.1	6.84 (1H, dd, 17.5, 10.9)	135.1	6.66 (1H, dd, 17.5, 10.9)	135.4	6.81 (1H, dd, 17.5, 10.9)
14	115.9	5.49 (1H, d, 10.9)	115.9	5.51 (1H, d, 10.9)	115.7	5.46 (1H, d, 10.9)	115.6	5.31 (1H, d, 10.9)	115.9	5.38 (1H, d, 10.9)
		6.07 (1H, d, 17.5)		6.09 (1H, d, 17.5)		6.02 (1H, d, 17.5)		5.85 (1H, d, 17.5)		5.97 (1H, d, 17.5)
1′	78.3	5.89 (1H, d, 9.6)	76.4	6.23 (1H, d, 9.6)	78.5	5.98 (1H, d, 9.6)	78.4	5.77 (1H, d, 9.6)	80.4	5.73 (1H, d, 9.3)
2′	70.6	4.15 (1H, overlapped)	74.1	5.35 (1H, t, 9.6)	67.6	4.42 (1H, t, 9.6)	70.5	4.03 (1H, t, 9.6)	68.8	3.93 (1H, m)
3′	76.2	3.82 (1H, dd, 9.2, 3.2)	73.8	4.01 (1H, dd, 9.6, 3.4)	79.0	5.09 (1H, dd, 9.6, 3.3)	74.3	3.91 (1H, overlapped)	42.4	1.71 (1H, q, 11.4)
										2.42 (1H, m)
4′	72.7	3.85 (1H, brd, 3.4)	72.7	3.90 (1H, brd, 3.4)	70.2	4.03 (1H, brd, 3.3)	74.6	5.23 (1H, brd, 3.5)	70.9	3.25 (1H, overlapped)
5′	74.8	4.38 (1H, q, 6.5)	75.1	4.28 (1H, q, 6.5)	74.3	4.45 (1H, q, 6.5)	73.1	4.40 (1H, q, 6.5)	78.5	3.86 (1H, m)
6′	15.8	1.26 (3H, d, 6.5)	15.6	1.37 (3H, d, 6.5)	15.7	1.25 (3H, d, 6.5)	15.7	0.98 (3H, d, 6.5)	16.8	1.12 (3H, d, 6.5)
1″			170.4		171.4		171.5			
2″			19.0	1.46 (3H, s)	19.7	2.19 (3H, s)	19.5	2.08 (3H, s)		
10-OCH_3	55.6	4.19 (3H, s)	55.6	4.20 (3H, s)	55.6	4.11 (3H, s)	55.5	3.91 (3H, s)	55.6	4.09 (3H, s)
12-OCH_3	55.6	4.17 (3H, s)	55.5	4.18 (3H, s)	55.4	4.08 (3H, s)	55.3	3.86 (3H, s)	55.6	4.08 (3H, s)

additional NOE correlations of H-3′a to both H-1′ and H-5′ and H-3′b to H-2′, indicating that H-3′a and H-3′b are in an axial and equatorial orientation, respectively (Figure 3A). Thus, the sugar moieties of the compounds were assigned to be the same relative configuration, matching that of reported ravidomycin analogs.

Assigning Sugar Absolute Configuration and Redefining $[\alpha]_D^{25}$ for Deacetylravidomycin. The specific rotations of the isolated compounds were compared to the data of reported ravidomycin analogs to determine their absolute configurations. Although the sign of the specific rotation of ravidomycin (**14**; $[\alpha]_D^{25}$ −15, MeCN) agreed with previous work ($[\alpha]_D^{25}$ −100, MeCN),[20] the specific rotation of the isolated deacetylravidomycin (**15**; $[\alpha]_D^{25}$ +11, $CHCl_3$/MeOH 1:1) was opposite that of a previous report of deacetylravidomycin isolated from *S. ravidus* ($[\alpha]_D^{25}$ −15, $CHCl_3$/MeOH 1:1).[6]

To test if *Streptomyces* Am59 produced a different deacetylravidomycin enantiomer than *S. ravidus*, we obtained commercially available deacetylravidomycin (Santa Cruz Biotechnology Inc., Dallas, TX, USA) isolated from *S. ravidus*. Like our sample, it yielded a positive specific rotation ($[\alpha]_D^{25}$ +71). We also obtained *S. ravidus* NRRL 11300 from the USDA stock center and fermented it using the procedure from the literature.[20] The specific rotation of the deacetylravidomycin isolated from *S. ravdius* NRRL 11300 also showed a positive sign ($[\alpha]_D^{25}$ +12). Therefore, we concluded that *Streptomyces* Am59 and *S. ravidus* produce the same enantiomer of deacetylravidomycin.

To verify that our isolated deacetylravidomycin (with positive specific rotation) has the reported absolute configuration (containing a D-ravidosamine), its ECD spectrum was obtained and compared to a calculated ECD spectrum. Time-dependent density functional theory (TDDFT) was used to generate theoretical ECD curves for the 55 lowest energy conformers of deacetylravidomycin (**15**; Figure S78). These theoretical ECD curves were weighted by their free energy to generate a single ECD curve, which matched the experimental ECD data (Figure 4A), indicating that compound **15** contains a D-ravidosamine, as reported for deacetylravidomycin. The ECD spectra of all of the compounds were measured and showed the same pattern, indicating that all new analogs have the same absolute configuration as the reported ravidomycin analogs.

https://doi.org/10.1021/acs.jnatprod.3c00381
J. Nat. Prod. 2023, 86, 1968−1979

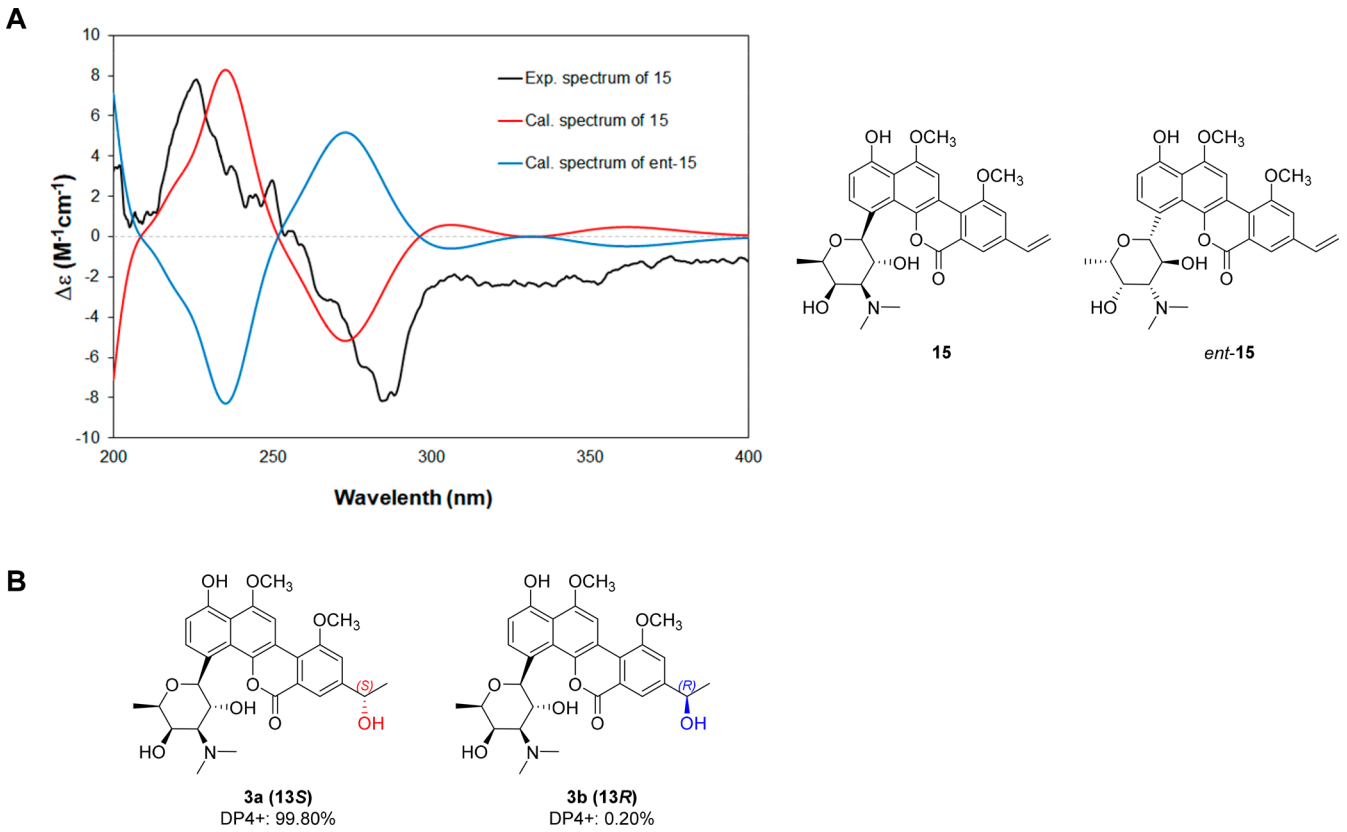

Figure 4. Computational analysis. (A) Comparison of the experimental and calculated ECD spectra of deacetylravidomycin. (B) Results of DP4+ analysis for **3a** (13*S*) and **3b** (13*R*).

Because our isolates of deacetylravidomycin match the reported absolute configuration but conflict with the reported specific rotation, we believe that the previous report of a negative specific rotation was in error. As additional support, we validated the positive specific rotation on a second polarimeter. Furthermore, we deacetylated ravidomycin by refluxing in methanol (Figure S79).[21] Again, this process yielded deacetylravidomycin with a positive specific rotation ($[\alpha]_D^{25}$ +14, MeCN) from ravidomycin with a negative specific rotation ($[\alpha]_D^{25}$ −15, MeCN). Therefore, we believe that deacetylravidomycin actually exhibits a negative specific rotation. Interestingly, this conclusion means that the presence of an acetyl group on the 4′ position reverses the sign of the specific rotation of ravidomycin. In fact, previous research has reported that ravidomycin diacetate also exhibits positive specific rotation ($[\alpha]_D^{25}$ +33.3).[20] Thus, the specific rotations of ravidomycin analogs differ depending on the degree of acetylation.

Assigning Absolute Configuration at C-13 of 3 as *S*. In order to define the configuration at C-13 of **3**, NMR chemical shift calculations using DFT and DP4+ statistical analysis were carried out. Before optimizing the structure of **3**, the configuration of the sugar moiety was confirmed to be consistent with that of **15** by NOESY data and its ECD spectrum. Thus, two probable diastereomers (**3a**, 13*S*; **3b**, 13*R*; Figure 4B) were established, and their ^{1}H and ^{13}C NMR chemical shifts were calculated with their Boltzmann averaged populations. Subsequently, calculated data of **3a** and **3b** were compared to the experimental data of **3**. The analysis resulted in a 99.8% probability for the experimental data of **3** to match **3a**, revealing that the absolute configuration of **3** should be *S* (Figures 4B and S80). This assignment is consistent with the *S*-configuration of C-13 in gilvocarcin HE,[7] suggesting that the aglycone undergoes the same modification en route to both compounds.

***Streptomyces* Am59 and *S. ravidus* Possess Nearly Identical Ravidomycin Biosynthetic Gene Clusters.** Given that *Streptomyces* sp. Am59 produced ravidomycin analogs that were previously unreported from *S. ravidus*, we hypothesized that the ravidomycin biosynthetic gene clusters would differ between the species. In particular, since the new ravidomycin analogs have different sugars, we expected either (a) differences in the glycosyltransferase making it more promiscuous or (b) additional enzymes that modify the sugar. However, sequencing of the *Streptomyces* sp. Am59 genome revealed a series of genes that are nearly identical to the published biosynthetic gene cluster of *S. ravidus* (Figure 5).[29] Analysis in AntiSMASH revealed that the genes have the same orientation, and their translated sequences share nearly 100% identity (Table 4).[30] The only major difference is that genes

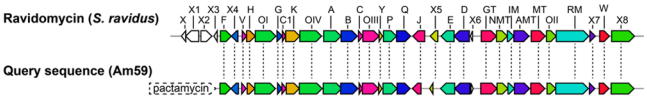

Figure 5. Ravidomycin biosynthetic gene clusters in *S. ravidus* and *Streptomyces* sp. Am59. Analysis in antiSMASH[30] revealed a biosynthetic gene cluster from *Streptomyces* sp. Am59 (bottom) with nearly 100% identity to the ravidomycin biosynthetic gene cluster of *S. ravidus* (top). Immediately adjacent to this cluster in Am59 was a cluster homologous to the pactamycin biosynthetic gene cluster of *S. pactum* (see Figure S81 and Table S1).

https://doi.org/10.1021/acs.jnatprod.3c00381
J. Nat. Prod. 2023, 86, 1968−1979

Table 4. Ravidomycin Biosynthetic Gene Cluster Comparison between *Streptomyces* sp. Am59 and and *S. ravidus*

S. ravidus gene name	homologue gene description	% ID
ravF	putative ketoreductase	100
ravX4	putative regulatory protein	100
ravV	hypothetical protein	100
ravH	putative NADPH-dependent FMN reductase	100
ravOI	putative monooxygenase	97
ravG	putative cyclase	100
ravC1	putative acyl carrier protein	99
ravK	putative aromatase/cyclase	100
ravOIV	putative oxygenase	97
ravA	putative ketoacyl synthase	99
ravB	putative chain length factor	99
ravC	putative acyl carrier protein	100
ravOIII	putative cytochrome p450 monooxygenase	100
ravY	putative ferrodoxin protein	99
ravP	putative acyltransferase	99
ravQ	putative acyltransferase	98
ravJ	hypothetical protein	99
ravX5	putative regulatory gene	99
ravE	NDP-glucose-4,6-dehydratase	99
ravD	putative NDP-glucose synthase	99
ravGT	putative C-glycosyltransferase	99
ravNMT	putative *N,N*-dimethyltransferase	99
ravIM	putative keto-isomerase	97
ravAMT	putative aminotransferase	99
ravMT	putative *O*-methyltransferase	99
ravOII	putative anthrone oxygenase	99
ravRM	putative dehydrogenase	97
ravX7	hypothetical protein	98
ravW	putative *N*-acetyltransferase	95
ravX8	hypothetical protein	99

ravX, *ravX1*, *ravX2*, and *ravX3* are absent from the *Streptomyces* sp. Am59 cluster. However, these genes had no predicted role in ravidomycin biosynthesis.[29] In place of these *ravX* genes, a pactamycin-like biosynthetic gene[31] cluster abuts the ravidomycin gene cluster in *Streptomyces* sp. Am59 (Figures 5 and S81, Table S1); however, we did not observe pactamycin in our LCMS data, and it is unclear how this adjacent gene cluster could help generate the new analogs.

Underscoring the similarity of the *S. ravidus* and Am59 gene clusters, the glycosyltransferase (RavGT) homologues have 99% identity. Furthermore, in other biosynthetic pathways, methyl carbamate moieties (present in **4** and **6**) are installed via oxidation of a methylamine and subsequent methylation of the carbamic acid.[32,33] However, no additional oxidoreductase or methyl transferase is present in the Am59 biosynthetic gene cluster. Finally, the RavAMT methyl transferases are also nearly identical, which offers no indication of a deficiency in installing the amine onto the sugar resulting in the fucose analogs (**9**–**13**). Therefore, the ravidomycin biosynthetic gene cluster does not provide an explanation for the production of new analogs by *Streptomyces* sp. Am59.

An alternative explanation is that RavGT is inherently promiscuous, and the relative abundance of activated sugar substrates determines which products form. This hypothesis is supported by an observation from Rohr and colleagues.[29] They deleted the glycosyltransferase gene from the gilvocarcin producer *S. lividans* and replaced it with the *S. ravidus ravGT* gene. They reported that RavGT did not append a ravidosamine, but instead it incorporated a fucofuranose—the sugar present in gilvocarcin. Therefore, RavGT may be a promiscuous glycosyltransferase, and *Streptomyces* sp. Am59 may possess an especially diverse pool of activated ravidosamines and fucopyranoses (at least under our fermentation conditions).

New Analogs Exhibit Selectively Decreased Potency Relative to Deacetylravidomycin. Given the known antimicrobial and cytotoxic activity of ravidomycin and its analogs, we tested the antiproliferative activity of the new analogs against three pathogenic micro-organisms and a cancer cell line (Table 5). The pathogens represent Gram-positive bacteria (*Staphylococcus aureus*), Gram-negative bacteria (*Pseudomonas aeruginosa*), and yeast (*Candida albicans*). The cancer cell line is a triple-negative breast cancer (HCC1806).

Table 5. Biological Activities of Isolated Compounds (1 and 3–17)

	MIC (μg/mL)			IC_{50} (nM)
compounds	*P. aeruginosa*	*S. aureus*	*C. albicans*	*HCC1806*
1	>13	0.39	13	>10 000
3	>13	13	>13	>10 000
4	50	0.003	6.3	550
5	50	0.006	13	1700
6	25	0.012	6.3	710
7	>13	0.10	13	>10 000
8	6.3	0.049	0.78	53
9	3.1	0.006	13	3600
10	>100	0.049	>25	870
11	>100	0.006	6.3	370
12	50	0.003	6.3	5100
13	50	0.10	6.3	>10 000
14	13	0.39	0.39	42
15	3.1	0.006	0.78	81
16	>100	0.78	25	>10 000
17	>100	1.6	100	3600

No new analogs were substantially more potent than deacetylravidomycin (compound **15**). Its singly methylated analog (**8**) exhibited comparable activity but was almost 10× less potent against *S. aureus*. In contrast, several analogs (**4**–**6**, **11**, and **12**) exhibited potency against *S. aureus* similar to that of **15** but were ∼10× weaker inhibitors of *P. aeruginosa*, *C. albicans*, and the breast cancer cells. These analogs shared an acetyl or methyl carbamoyl modification of the amine at the C-3′ position, except for **12**, which was acetylated at the C-4′ position.

Compound **9**, which possesses a D-fucopyranose sugar without any acetylation was notably selective against bacteria (*P. aeruginosa* and *S. aureus*) relative to eukaryotes (*C. albicans* and HCC1806). The OH-3′ is essential for the antibacterial potency, demonstrated by ∼20× loss of antibacterial potency by compound **13**. Compound **9** was previously prepared by chemical synthesis and shown to have antimycobacterial effects, but we are not aware of work illustrating its lack of potency against yeast and human cells. Intriguingly, this selectivity complements that of ravidomycin (**14**), which is more potent against eukaryotes than prokaryotes.

Compounds **3**, **16**, and **17** lack the styrene moiety and are much less potent than styrene-containing analogs (in agreement with previous work).[7] Also in agreement with previous

https://doi.org/10.1021/acs.jnatprod.3c00381
J. Nat. Prod. 2023, 86, 1968−1979

work, compound **1** lacks methylation at the C-10 position and is universally less potent.[6]

CONCLUSION

In total, we have characterized 10 new analogs of the antibiotic ravidomycin, and we reported the first isolation of fucomycin V from a natural source. Our results also indicate that the specific rotation for deacetylravidomycin carries a positive sign instead of the previously reported negative value. Finally, we characterized several modifications that altered the biological activity of deacetylravidomycin: (a) acetylation and carbamoylation of the amino group of the ravidosamine decreased potency to all organisms *except* the Gram-positive bacterium *S. aureus*, (b) replacement of the ravidosamine with a D-fucopyranose afforded increased selectivity against bacteria (both Gram-positive and Gram-negative), and (c) modification or removal of the styrene moiety universally inactivates these toxins. Together, these findings expand our knowledge of naturally occurring angucycline antibiotics.

EXPERIMENTAL SECTION

General Experimental Procedures. Optical rotations were measured with a PerkinElmer model 343 polarimeter. UV spectra were obtained from HPLC data. ECD spectra were recorded with a JASCO J-715 CD spectrometer. 1D (^{1}H and ^{13}C) and 2D (COSY, HSQC, HMBC, and NOESY) NMR spectra were recorded on a Bruker 500 MHz Avance Neo NMR spectrometer. Spectra were referenced to the methanol-d_4 solvent peaks (δ_C 49.0; δ_H 3.31). Unless stated otherwise, high resolution electrospray ionization mass spectrometry (HR-ESI-MS) data were obtained using a Thermo Fisher Orbitrap Fusion Lumos Tribrid mass spectrometer. Low resolution liquid chromatography mass spectrometry (LR-LC-MS) data were obtained using an Agilent LC/MSD XT single quadrupole LC-MS coupled to an Agilent 1260 Infinity II HPLC systems and a Phenomenex Synergi 4 μm Hydro-RP 80 Å column (250 × 4.6 mm) with a water/acetonitrile linear gradient containing 0.1% formic acid at 0.7 mL/min. The isolation and purification of metabolites was carried out using an Agilent 1260 Infinity II HPLC system with Phenomenex Luna 5 μm C8(2) 100 Å and Synergi 4 μm Hydro-RP 80 Å (250 × 10 mm) columns.

Biological Material. Fungal specimens were collected in February, 2017, in the Amazon Forest, Brazil (2°32′4″ S, 60°50′11″ W) under SisGen registration number AC0DE2E. For cultivation, a sample of fungus was macerated and diluted in buffer. Dilutions were plated on chitin agar [agar (20 g/L), chitin (4 g/L), K_2HPO_4 (0.77 g/L), $MgSO_4$-$7H_2O$ (0.5 g/L), KH_2PO_4 (0.37 g/L), $FeSO_4$-$7H_2O$ (0.01 g/L), $MnCl_2$-$4H_2O$ (0.001 g/L), $ZnSO_4$-$7H_2O$ (0.001 g/L)] supplemented with 50 μg/mL cycloheximide and 50 μg/mL nystatin. Plates were incubated at 30 °C for 3 weeks. Colonies were restreaked to purity on ISP2 agar plates.

Initial Metabolite Production by *Streptomyces* sp. Am59. *Streptomyces* Am59 was separately incubated in three different liquid growth media [YEME: yeast extract (4 g/L), malt extract (10 g/L), dextrose (4 g/L); A-medium: yeast extract (5 g/L), peptone (5 g/L), dextrose (10 g/L), soluble starch (20 g/L), $CaCO_3$ (5 g/L); RAM2: corn meal (4 g/L), dextrose (10 g/L), maltose (15 g/L), cottonseed flour (7.5 g/L), dry yeast (5 g/L)]. Each culture contained 1 L of media and 50 g of total prewashed resin mix (30 g of HP20, 10 g of Amberlite XAD7HP, 10 g of Amberlite XAD4). The cultures were fermented in 4 L Erlenmeyer flasks at 30 °C with 150 rpm orbital shaking for 18 days. Then, the resin from all three flasks was collected, washed with water, and combined. The combined resin was extracted sequentially with ∼500 mL of methanol and ∼500 mL of acetone for ∼6 h each. These extracts were combined and dry-loaded onto 4 g of Celite before fractionation through 8.5 g of C8 resin [Phenomenex Sepra, 50 μm, 65 Å, #04K-4406]. This fractionation was performed on a Teledyne ISCO Combiflash RF+ instrument using the following step gradient: 40 mL each of water, 15% MeCN in H_2O, 30% MeCN in H_2O, 45% MeCN in H_2O, 60% MeCN in H_2O, 80% MeCN in H_2O, MeCN, repeated MeCN. The final four of the eight fractions were each redissolved in DMSO to a concentration of 10 mg/mL. Then, 2 μL of each of the four fractions was added to 80 μL of 50% MeCN in H_2O. The soluble supernatant was used for LC-MS/MS analysis.

Initial LC-MS/MS Analysis of *Streptomyces* sp. Am59 Extract. High-resolution electrospray ionization (HR-ESI) mass spectra with collision-induced dissociation (CID) MS/MS were obtained using an Agilent LC-q-TOF mass spectrometer 6530 equipped with an Agilent 1290 uHPLC system. Metabolites were separated using a Kinetex 2.6 μm C8 (100 × 2.1 mm) column [P/N 00D-4497-AN]. Mobile phase A was water containing 0.1% formic acid. Mobile phase B was acetonitrile. After initially holding 30% phase B for 1 min, a linear gradient was applied to 100% mobile phase B over 12.5 min. Data-dependent acquisition was employed to fragment the top three masses in each scan. An exclusion list was employed that contained features that were present in the three nutrient media (YEME, A-medium, and RAM2), and an active exclusion was employed to avoid fragmenting the same ion more than twice in a 2 min range. Collision-induced dissociation was applied using a linear formula that applied a higher voltage for larger molecules (CID voltage = 10 + 0.02 m/z).

Molecular Networking Analysis. The LC-MS/MS data were exported as an .mgf file from Agilent MassHunter Qualitative Analysis software. This file was uploaded into GNPS (https://gnps.ucsd.edu/ProteoSAFe/static/gnps-splash.jsp) and used to generate a molecular network with the following settings: Precursor ion mass tolerance 0.02 Da, fragment ion mass tolerance 0.02 Da, min pairs cos 0.65, min matched fragment ions 4, maximum shift 1999 Da, min cluster size 2, network TopK 10, max connected component size 100. The resulting network was visualized in Cytoscape (https://cytoscape.org/).

Bacterial Fermentation. *Streptomyces* sp. Am59 was grown into sporulated colonies on a YEME agar plate [yeast extract (4 g/L), malt extract (10 g/L), and dextrose (4 g/L) in 1 L of distilled water and 1.5% agar] for 5 days at 30 °C. A single colony of solid culture was scraped and seeded into 4 mL of YEME medium in a culture tube, and the culture was grown with 220 rpm orbital rotation for 5 days at 30 °C. This culture was used to inoculate three larger cultures (1 mL into 100 mL fresh YEME) in 500 mL Erlenmeyer flasks and incubated with 220 rpm rotation for 7 days at 30 °C. Finally, 27 1-L cultures of A-medium containing 70 g of mixed resin (Amberlite XAD-7HP/XAD4/HP20 = 1:1:2) in 4 L Erlenmeyer flasks was inoculated by 10 mL of one of the three medium-scale cultures and incubated with 180 rpm orbital agitation for 10 days at 30 °C.

Extraction and Isolation. Each of the 27 1-L cultures of *Streptomyces* sp. Am59 was filtered through a Büchner funnel with Miracloth under vacuum to collect the resin. The recovered resin mixture was successively soaked in 6 L of MeOH and 6 L of acetone with stirring for 3 h. The extracts were filtered using a Büchner funnel with a filter paper, and 84 g of Celite adsorbent was added and dried under reduced pressure. The dried extract-coated Celite (200 g) was loaded onto a silica gel column (180 g) and separated using a step gradient ($CHCl_3$/MeOH, 25:1, 10:1, 5:1, 2:1, 1:1, and 100% MeOH) to give six fractions (A−F). Fraction A (8.7 g) was redissolved in MeOH and fractionated using prep HPLC with a Phenomenex Luna 10 μm C8(2) 100 Å (250 × 21.2 mm, flow rate 8.0 mL/min) column with a gradient elution from 10 to 100% aqueous acetonitrile over 60 min using a 75 s fraction collection time window. Fraction A15 was purified by HPLC with isocratic elution (Luna 10 μm C8(2), 45% MeOH) to give **1** (0.5 mg), **3** (0.5 mg), **15** (2.3 mg), **16** (3.0 mg), and **17** (3.3 mg). Fraction A16 was purified by HPLC with isocratic elution (Luna 10 μm C8(2), 47% MeOH) to give **2** (0.6 mg), **14** (2.0 mg), and **8** (0.5 mg). Fractions A22−A25 were purified by gradient HPLC using a Synergi 4 μm Hydro-RP column. Fraction A22 was separated using a 30−45% ACN gradient to give **7** (0.5 mg) and **9** (0.8 mg). Fraction A23 was separated using a 60−90% MeOH gradient to give **5** (2.9 mg). Fraction A24 was separated using a 60−70% MeOH gradient to give **6** (0.8 mg) and **13** (1.2 mg). Fraction

https://doi.org/10.1021/acs.jnatprod.3c00381
J. Nat. Prod. 2023, 86, 1968−1979

A25 was separated using a 60−90% MeOH gradient to give **4** (3.2 mg), **10** (0.7 mg), **11** (1.9 mg), and **12** (4.9 mg).

*10-O-Demethyl-deacetylravidomycin (**1**).* Yellow amorphous gum. $[\alpha]_D^{25}$ +12 (*c* 0.1, MeOH). UV (MeOH): λ_{max} (log ε) 252 (2.54), 288 (2.59) nm. ECD (2.0 mM, MeOH): λ_{max} ($\Delta\varepsilon$) 226 (+7.7), 284 (−8.1) nm. ^{1}H (500 MHz) and ^{13}C (125 MHz) NMR data in CD_3OD, see Tables 1 and 2. HR-ESI-MS (positive-ion mode): *m*/*z* 508.1961 $[M + H]^+$ (calcd for $C_{28}H_{30}NO_8$, 508.1966).

*Ravidomycin M (**2**).* Yellow amorphous gum. UV (MeOH): λ_{max} (log ε) 246 (2.19), 276 (2.04) nm. ECD (1.8 mM, MeOH): λ_{max} ($\Delta\varepsilon$) 226 (+6.9), 284 (−7.3) nm. ^{1}H (500 MHz) and ^{13}C (125 MHz) NMR data in CD_3OD, see Tables 1 and 2. HR-ESI-MS (positive-ion mode) *m*/*z*: 552.2230 $[M + H]^+$ (calcd for $C_{30}H_{34}NO_9$: 552.2228).

*Deacetylravidomycin HE (**3**).* Yellow amorphous gum. $[\alpha]_D^{25}$ +7 (*c* 0.1, MeOH). UV (MeOH): λ_{max} (log ε) 246 (2.49), 275 (2.34) nm. ECD (1.9 mM, MeOH): λ_{max} ($\Delta\varepsilon$) 226 (+7.5), 284 (−8.0) nm. ^{1}H (500 MHz) and ^{13}C (125 MHz) NMR data in CD_3OD, see Tables 1 and 2. HR-ESI-MS (positive-ion mode): *m*/*z* 540.2225 $[M + H]^+$ (calcd for $C_{29}H_{34}NO_9$: 540.2228).

*N-Demethyl-N-methoxycarbonyl-deacetylravidomycin (**4**).* Yellow amorphous gum. $[\alpha]_D^{25}$ −23 (*c* 0.1, MeOH). UV (MeOH): λ_{max} (log ε) 253 (2.23), 288 (2.27) nm. ECD (1.8 mM, MeOH): λ_{max} ($\Delta\varepsilon$) 226 (+7.0), 284 (−7.3) nm. ^{1}H (500 MHz) and ^{13}C (125 MHz): NMR data in CD_3OD, see Tables 1 and 2. HR-ESI-MS (positive-ion mode): *m*/*z* 566.2020 $[M + H]^+$ (calcd for $C_{30}H_{32}NO_{10}$: 566.2021).

*FE35A (**5**).* Yellow amorphous gum. $[\alpha]_D^{25}$ +12 (*c* 0.1, MeOH). UV (MeOH): λ_{max} (log ε) 251 (2.19), 287 (2.24) nm. ECD (1.8 mM, MeOH): λ_{max} ($\Delta\varepsilon$) 226 (+7.2), 284 (−7.6) nm. ^{1}H (500 MHz) and ^{13}C (125 MHz) NMR data in CD_3OD, see Tables 1 and 2. HR-ESI-MS (positive-ion mode): *m*/*z* 550.2070 $[M + H]^+$ (calcd for $C_{30}H_{32}NO_9$: 550.2072).

*N,N-Didemethyl-N-methoxycarbonyl-deacetylravidomycin (**6**).* Yellow amorphous gum. $[\alpha]_D^{25}$ +12 (*c* 0.1, MeOH). UV (MeOH) λ_{max} (log ε) 252 (2.23), 288 (2.26) nm. ECD (1.8 mM, MeOH): λ_{max} ($\Delta\varepsilon$) 226 (+7.2), 284 (−7.5) nm. ^{1}H (500 MHz) and ^{13}C (125 MHz) NMR data in CD_3OD, see Tables 1 and 2. HR-ESI-MS (positive-ion mode): *m*/*z* 552.1865 $[M + H]^+$ (calcd for $C_{29}H_{30}NO_{10}$: 552.1864).

*N,N-Didemethyl-N-acetyl-deacetylravidomycin (**7**).* Yellow amorphous gum; $[\alpha]_D^{25}$ +32 (*c* 0.05, MeOH). UV (MeOH): λ_{max} (log ε) 251 (2.54), 288 (2.59) nm. ECD (1.9 mM, MeOH): λ_{max} ($\Delta\varepsilon$) 226 (+7.6), 284 (−8.1) nm. ^{1}H (500 MHz) and ^{13}C (125 MHz) NMR data in CD_3OD, see Tables 1 and 2. HR-ESI-MS (positive-ion mode): *m*/*z* 536.1913 $[M + H]^+$ (calcd for $C_{29}H_{30}NO_9$: 536.1915).

*Fucomycin V (**9**).* Yellow amorphous gum. $[\alpha]_D^{25}$ +6 (*c* 0.05, MeOH). UV (MeOH) λ_{max} (log ε) 252 (2.22), 287 (2.26) nm. ECD (2.0 mM, MeOH): λ_{max} ($\Delta\varepsilon$) 226 (+7.7), 284 (−8.2) nm. ^{1}H (500 MHz) and ^{13}C (125 MHz) NMR data in CD_3OD, see Table 3. HR-ESI-MS (positive-ion mode): *m*/*z* 495.1646 $[M + H]^+$ (calcd for $C_{27}H_{27}O_9$: 495.1650).

*2′-Acetyl-fucomycin V (**10**).* Yellow amorphous gum. $[\alpha]_D^{25}$ +30 (*c* 0.1, MeOH). UV (MeOH): λ_{max} (log ε) 252 (2.52), 287 (2.57) nm. ECD (1.9 mM, MeOH): λ_{max} ($\Delta\varepsilon$) 226 (+7.5), 284 (−7.8) nm. ^{1}H (500 MHz) and ^{13}C (125 MHz) NMR data in CD_3OD, see Table 3. HR-ESI-MS (positive-ion mode): *m*/*z* 537.1757 $[M + H]^+$ (calcd for $C_{29}H_{29}O_{10}$: 537.1755).

*3′-Acetyl-fucomycin V (**11**).* Yellow amorphous gum. $[\alpha]_D^{25}$ +25 (*c* 0.1, MeOH). UV (MeOH): λ_{max} (log ε) 252 (2.23), 288 (2.26) nm. ECD (1.9 mM, MeOH): λ_{max} ($\Delta\varepsilon$) 226 (+7.7), 284 (−8.0) nm. ^{1}H (500 MHz) and ^{13}C (125 MHz) NMR data in CD_3OD, see Table 3. HR-ESI-MS (positive-ion mode): *m*/*z* 537.1757 $[M + H]^+$ (calcd for $C_{29}H_{29}O_{10}$, 537.1755).

*4′-Acetyl-fucomycin V (**12**).* Yellow amorphous gum. $[\alpha]_D^{25}$ −23 (*c* 0.1, MeOH). UV (MeOH): λ_{max} (log ε) 252 (2.20), 288 (2.28) nm. ECD (1.9 mM, MeOH): λ_{max} ($\Delta\varepsilon$) 226 (+7.9), 284 (−8.3) nm. ^{1}H (500 MHz) and ^{13}C (125 MHz) NMR data in CD_3OD, see Table 3. HR-ESI-MS (positive-ion mode): *m*/*z* 537.1758 $[M + H]^+$ (calcd for $C_{29}H_{28}O_{10}$: 537.1755).

*3′-Deoxy-fucomycin V (**13**).* Yellow amorphous gum. $[\alpha]_D^{25}$ −18 (*c* 0.1, MeOH). UV (MeOH): λ_{max} (log ε) 252 (2.19), 288 (2.26) nm. ECD (2.1 mM, MeOH): λ_{max} ($\Delta\varepsilon$) 226 (+7.2), 284 (−7.7) nm. ^{1}H (500 MHz) and ^{13}C (125 MHz) NMR data in CD_3OD, see Table 3. HR-ESI-MS (positive-ion mode): *m*/*z* 479.1700 $[M + H]^+$ (calcd for $C_{27}H_{27}O_8$: 479.1700).

Computational Analysis. All electronic structure calculations were performed using the Gaussian 16 program suite.[34] To obtain initial geometries of each species considered in this work, a molecular mechanics (MM) conformational search was performed using the GMMX algorithm in Gaussian with the MMFF94 force field and an energy window of 7 kcal/mol. For the ECD calculations, conformers obtained in the previous step were further optimized with quantum mechanical (QM) methods, using the long-range, dispersion corrected ωB97X-D functional and the 6-311++G(d,p) Pople basis set.[35−37] Frequency calculations performed at the same level of theory verified that each conformer was a minimum. Optimization and frequency were performed directly in methanol using the SMD solvation model. ECD calculations were carried out on the resultant geometries by the TDDFT method at the ωB97X-D/def2-TZVP level in methanol using the SMD solvation model.[38,39] The calculated ECD curve was generated using SpecDis 1.71,[40] in which contributions from the 55 conformers were weighted by Gibbs free energy.

The DP4+ protocol outlined in the work by Zanardi and Sarotti et al. was followed for the NMR calculations.[41] As suggested in their work, geometries obtained from the MM conformational search were further optimized using the B3LYP functional and 6-31G(d) basis set in the gas phase.[42,43] Frequency calculations were performed to ensure that each conformer was a minimum. Chemical shifts were then obtained by performing GIAO NMR calculations at the mPW1PW91/6-31+G(d,p) level using the PCM solvation model for TMS and the two diastereomers.[44,45] For each diastereomer, duplicate conformers were discarded, and Boltzmann weighted chemical shifts were calculated. These Boltzmann weighted chemical shifts were then used in the DP4+ analysis.

Antibacterial and Antifungal Assays. *Staphylococcus aureus* strain Newman[46] and *Pseudomonas aeruginosa* PAO1 (Δ*mexA-BoprM*)[47] were cultured in Mueller-Hinton Broth. *Candida albicans* strain SC5314[48] was cultured in RPMI 1640 medium (Sigma R7388) supplemented with 165 mM morpholinepropane-sulfonic acid (MOPS) and adjusted to pH 7.0. For all three, overnight cultures were diluted 1:1000 into fresh media, and 200 μL of these cultures was added to wells of 96-well microtiter plates, which already contained 2 μL of a DMSO solution of the test compound. Plates were subsequently incubated at room temperature under room fluorescent lighting for 24 h. Then, their OD600 was read (BioTek Synergy H1 plate reader). Minimal inhibitory concentrations were defined as the lowest concentration that prevented the OD600 from rising above 0.1.

Cell Viability Assays. HCC1806 cells were maintained in DMEM (Gibco, Thermo Fisher Scientific) supplemented with 10% FBS, 100 U/mL penicillin and 100 μg/mL streptomycin, and 1% GlutaMax supplement (Thermo Fisher). Cells were originally obtained from the Lineberger Comprehensive Cancer Center (UNC Chapel Hill). Cells are routinely tested for mycoplasma contamination and were cultured no more than 4 weeks for experiments.

HCC1806 cells were seeded onto 96-well plates at a density of 2500 cells per well. Twenty-four hours later, media were replaced with 0.1% DMSO (vehicle) or the indicated concentration of compound (six wells per dose). Seventy-two hours later, viability was determined by Promega Cell Titer Glo 2.0 assay. Luminescence values were read on a BioTek Synergy H4 plate reader (Agilent) and data plotted as percent viability relative to DMSO (vehicle) using GraphPad Prism 9.3.1. The IC_{50} values were determined in Prism from the log (inhibitor) vs normalized response least-squares fit function.

Genome Sequencing and Assembly. Genomic DNA of *Streptomyces* sp. Am59 was extracted from the mycelium cultivated in 4 mL of YEME medium using the Wizard Genomic DNA Purification Kit (Promega). Approximately 100 ng of the gDNA was used for library preparation following the protocol of the NEXTFLEX

https://doi.org/10.1021/acs.jnatprod.3c00381
J. Nat. Prod. 2023, 86, 1968−1979

Rapid DNA-Seq kit. The final library concentration and distribution was analyzed using the Agilent D1000 screen tape. The library was sequenced on a NextSeq500 PE run using a 150-cycle mid sequencing kit. Runs were demultiplexed with bcl2fastq v2.20.0.422.

Quality and adapter trimming was performed with fastp (v 0.21.0)[49] with these parameters: -l 30 -g -p. Assembly was performed with SPAdes.py (v3.15.2)[50] with these parameters: -t 38 -isolate. Identification of the biosynthetic cluster relied on the *Streptomyces ravidus* ravidomycin biosynthetic gene cluster reference sequence (Genbank ID FN565485.1) and was performed with NCBI blastall (v2.2.26)[51] with these parameters: -p blastn -F F -e 1e-30 -a 10 -X 1500 -m 8. The contigs identified had HSPs with 90%+ identity to the reference sequence. Assembly of the Sbv2 data was performed on the combined single-end and paired-end data with SPAdes.py (v3.15.3)[50] with these parameters: -isolate -k 21,33,55. The final assembly and raw sequence reads are available for download from the NCBI [Genbank BioProject accession no. PRJNA966938, Genome accession no. JASCAT000000000].

■ ASSOCIATED CONTENT

Supporting Information

The Supporting Information is available free of charge at https://pubs.acs.org/doi/10.1021/acs.jnatprod.3c00381.

HRESIMS and NMR data of compounds **1**−**7** and **9**−**13**, conformations used for ECD calculation of compound **15**, HPLC trace of ravidomycin deacetylation, DP4+ results, and dose−response curves of biological assays (PDF)

■ AUTHOR INFORMATION

Corresponding Authors

Kyoung Jin Park − *Department of Chemistry, Indiana University, Bloomington, Indiana 47405, United States;* Present Address: School of Pharmacy, Sungkyunkwan University, Suwon 16419, Republic of Korea. E-mail: pkjin6515@skku.edu; Email: kp39@iu.edu

Joseph P. Gerdt − *Department of Chemistry, Indiana University, Bloomington, Indiana 47405, United States;* orcid.org/0000-0002-0375-4110; Email: jpgerdt@iu.edu

Authors

Sarah Maier − *Department of Chemistry, Indiana University, Bloomington, Indiana 47405, United States*

Chengqian Zhang − *Department of Chemistry, Indiana University, Bloomington, Indiana 47405, United States*

Shelley A. H. Dixon − *Department of Pediatrics, Herman B. Wells Center for Pediatric Research, Indiana University School of Medicine, Indianapolis, Indiana 46202, United States*

Douglas B. Rusch − *Center for Genomics and Bioinformatics, Indiana University, Bloomington, Indiana 47405, United States*

Monica T. Pupo − *School of Pharmaceutical Sciences of Ribeirao Preto, University of São Paulo, Ribeirao Preto, São Paulo 05508-220, Brazil;* orcid.org/0000-0003-2705-0123

Steven P. Angus − *Department of Pediatrics, Herman B. Wells Center for Pediatric Research, Indiana University School of Medicine, Indianapolis, Indiana 46202, United States*

Complete contact information is available at: https://pubs.acs.org/10.1021/acs.jnatprod.3c00381

Funding

The research was supported by an NIH grant (R35GM138376 to J.P.G). K.J.P., S.P.A., and the Laboratory for Biological Mass Spectrometry were supported by the Indiana University Precision Health Initiative. S.M. was supported by the NSF (CHE-2102583). The 500 MHz NMR spectrometer of the Indiana University NMR facility was supported by NSF grant CHE-1920026, and the Prodigy probe was purchased in part with support from the Indiana Clinical and Translational Sciences Institute funded, in part, by NIH Award TL1TR002531. Funding for bacterial isolation was provided by the NIH (U19TW009872 and U19AI109673) and by the São Paulo Research Foundation (FAPESP 2013/50954-0).

Notes

The authors declare no competing financial interest.

■ ACKNOWLEDGMENTS

We thank E. Mevers and J. Clardy for isolation of the bacterial strain. We thank E. Mevers for independent validation of optical rotation measurements. We thank the USDA-ARS Culture Collection (NRRL) for providing a standard ravidomycin-producing bacterial strain. The research was supported by an NIH grant (R35GM138376 to J.P.G). K.J.P., S.P.A., and the Laboratory for Biological Mass Spectrometry were partially supported by the Indiana University Precision Health Initiative. S.M. was supported by the NSF (CHE-2102583). The 500 MHz NMR spectrometer of the Indiana University NMR facility was supported by NSF grant CHE-1920026, and the Prodigy probe was purchased in part with support from the Indiana Clinical and Translational Sciences Institute funded, in part, by NIH Award TL1TR002531. The Big Red 3 supercomputing facility at Indiana University was used for most of the calculations in this study. Funding for bacterial isolation was provided by the NIH (U19TW009872 and U19AI109673) and by the São Paulo Research Foundation (FAPESP 2013/50954-0).

■ REFERENCES

(1) Kharel, M. K.; et al. *Nat. Prod. Rep.* **2012**, *29*, 264−325.
(2) Kharel, M. K.; Rohr, J. *Curr. Opin. Chem. Biol.* **2012**, *16*, 150−61.
(3) Greenstein, M.; Monji, T.; Yeung, R.; Maiese, W. M.; White, R. J. *Antimicrob. Agents Chemother.* **1986**, *29*, 861−6.
(4) Takahashi, K.; Yoshida, M.; Tomita, F.; Shirahata, K. *J. Antibiot.* **1981**, *34*, 271−5.
(5) Yamashita, N.; Shin-ya, K.; Furihata, K.; Hayakawa, Y.; Seto, H. *J. Antibiot.* **1998**, *51*, 1105−8.
(6) Arai, M.; et al. *J. Antibiot.* **2001**, *54*, 562−6.
(7) Hou, J.; et al. *J. Antibiot.* **2012**, *65*, 523−6.
(8) Jain, S. K.; Pathania, A. S.; Parshad, R.; Raina, C.; Ali, A.; Gupta, A. P.; Kushwaha, M.; Aravinda, S.; Bhushan, S.; Bharate, S. B.; Vishwakarma, R. A. *RSC Adv.* **2013**, *3*, 21046.
(9) Wada, S. I.; et al. *J. Antibiot.* **2017**, *70*, 1078−1082.
(10) Wu, F.; et al. *ACS Cent. Sci.* **2020**, *6*, 928−938.
(11) Liu, T.; et al. *ChemBioChem.* **2009**, *10*, 278−86.
(12) Li, Y. Q.; et al. *Org. Biomol. Chem.* **2008**, *6*, 3601−5.
(13) McGee, L. R.; Misra, R. *J. Am. Chem. Soc.* **1990**, *112*, 2386−2389.
(14) Oyola, R.; Arce, R.; Alegria, A. E.; Garcia, C. *Photochem. Photobiol.* **1997**, *65*, 802−10.
(15) Sehgal, S. N.; Vezina, C. Ravidomycin and process of preparation. US4230692A, 1980.
(16) Findlay, J. A.; Liu, J.-S.; Radics, L.; Rakhit, S. *Can. J. Chem.* **1981**, *59*, 3018−3020.
(17) Narita, T.; et al. *J. Antibiot.* **1989**, *42*, 347−56.
(18) Futagami, S.; et al. *Tetrahedron Lett.* **2000**, *41*, 1063−1067.

(19) Ben, A.; Hsu, D.-S.; Matsumoto, T.; Suzuki, K. *Tetrahedron* **2011**, *67*, 6460−6468.
(20) Sehgal, S. N.; et al. *J. Antibiot.* **1983**, *36*, 355−61.
(21) Rakhit, S.; Eng, C.; Baker, H.; Singh, K. *J. Antibiot.* **1983**, *36*, 1490−4.
(22) Wang, M.; et al. *Nat. Biotechnol.* **2016**, *34*, 828−837.
(23) van Santen, J. A.; et al. *ACS Cent. Sci.* **2019**, *5*, 1824−1833.
(24) Weiss, U.; Yoshihira, K.; Highet, R. J.; White, R. J.; Wei, T. T. *J. Antibiot.* **1982**, *35*, 1194−201.
(25) Stewart, W. E.; Siddall, T. H. *Chem. Rev.* **1970**, *70*, 517−551.
(26) Johns, S. R.; Lamberton, J. A.; Sioumis, A. A. *Chem. Commun. (London)* **1966**, 480.
(27) Narita, M.; et al. Preparation of the antibiotic SS 50905 B from *Streptomyces ravidus*. JP62226981, 1987.
(28) Findlay, J. A.; Liu, J.-S.; Radics, L. *Can. J. Chem.* **1983**, *61*, 323−327.
(29) Kharel, M. K.; Nybo, S. E.; Shepherd, M. D.; Rohr, J. *ChemBioChem.* **2010**, *11*, 523−32.
(30) Medema, M. H.; et al. *Nucleic Acids Res.* **2011**, *39*, W339−46.
(31) Kudo, F.; Kasama, Y.; Hirayama, T.; Eguchi, T. *J. Antibiot.* **2007**, *60*, 492−503.
(32) Zhang, C.; Ding, W.; Qin, X.; Ju, J. *Mar. Drugs* **2019**, *17*, 593.
(33) Zhang, H.; et al. *J. Am. Chem. Soc.* **2007**, *129*, 14670−83.
(34) Frisch, M. J.; et al. *Gaussian 16*, Rev. A.03; Gaussian, Inc.: Wallingford, CT, 2016.
(35) Chai, J. D.; Head-Gordon, M. *Phys. Chem. Chem. Phys.* **2008**, *10*, 6615−20.
(36) Grimme, S.; Antony, J.; Ehrlich, S.; Krieg, H. *J. Chem. Phys.* **2010**, *132*, 154104.
(37) Grimme, S.; Ehrlich, S.; Goerigk, L. *J. Comput. Chem.* **2011**, *32*, 1456−65.
(38) Marenich, A. V.; Cramer, C. J.; Truhlar, D. G. *J. Phys. Chem. B* **2009**, *113*, 6378−96.
(39) Pescitelli, G.; Bruhn, T. *Chirality* **2016**, *28*, 466−74.
(40) Bruhn, T.; Schaumloffel, A.; Hemberger, Y.; Bringmann, G. *Chirality* **2013**, *25*, 243−9.
(41) Grimblat, N.; Zanardi, M. M.; Sarotti, A. M. *J. Org. Chem.* **2015**, *80*, 12526−34.
(42) Zanardi, M. M.; Sarotti, A. M. *J. Org. Chem.* **2021**, *86*, 8544−8548.
(43) Marcarino, M. O.; Cicetti, S.; Zanardi, M. M.; Sarotti, A. M. *Nat. Prod. Rep.* **2022**, *39*, 58−76.
(44) Adamo, C.; Barone, V. *J. Chem. Phys.* **1998**, *108*, 664−675.
(45) Tomasi, J.; Mennucci, B.; Cammi, R. *Chem. Rev.* **2005**, *105*, 2999−3093.
(46) Duthie, E. S.; Lorenz, L. L. *J. Gen. Microbiol.* **1952**, *6*, 95−107.
(47) Li, X. Z.; Nikaido, H.; Poole, K. *Antimicrob. Agents Chemother.* **1995**, *39*, 1948−53.
(48) Gillum, A. M.; Tsay, E. Y.; Kirsch, D. R. *Mol. Gen. Genet.* **1984**, *198*, 179−82.
(49) Chen, S.; Zhou, Y.; Chen, Y.; Gu, J. *Bioinformatics* **2018**, *34*, i884−i890.
(50) Prjibelski, A.; Antipov, D.; Meleshko, D.; Lapidus, A.; Korobeynikov, A. *Current Protocols in Bioinformatics* **2020**, *70*, e102.
(51) Altschul, S. F.; et al. *Nucleic Acids Res.* **1997**, *25*, 3389−402.

https://doi.org/10.1021/acs.jnatprod.3c00381
J. Nat. Prod. 2023, 86, 1968−1979